A plant-specific calreticulin is a key retention factor for a defective brassinosteroid receptor in the endoplasmic reticulum

Hua Jin[1], Zhi Hong, Wei Su, and Jianming Li[2]

Department of Molecular, Cellular, and Developmental Biology, University of Michigan, Ann Arbor, MI 48109-1048

Communicated by Joanne Chory, The Salk Institute for Biological Studies, La Jolla, CA, June 4, 2009 (received for review May 11, 2009)

Mammalian calreticulin (CRT) is a multifunctional Ca^{2+}-binding protein involved in more than 40 cellular processes in various subcellular compartments, such as Ca^{2+} storage and protein folding in the endoplasmic reticulum (ER). CRT homologues were discovered in plants almost 15 years ago, and recent studies revealed that many plant species contain 2 or more CRTs that are members of 2 distinct families, the CRT1/2 family and the plant-specific CRT3 family. However, little is known about their physiological functions. Here we report *ebs2* (*EMS-mutagenized bri1 suppressor 2*) as an allele-specific suppressor of *bri1–9*, a dwarf Arabidopsis mutant caused by retention of a defective brassinosteroid receptor in the ER. *EBS2* encodes the Arabidopsis CRT3 that interacts with ER-localized bri1–9 in a glycan-dependent manner. Loss-of-function *ebs2* mutations compromise ER retention of bri1–9 and suppress its dwarfism, whereas *EBS2* over-expression enhances its dwarf phenotype. In contrast, mutations of 2 other CRTs or their membrane-localized homologues calnexins had little effect on *bri1–9*. A domain-swapping experiment revealed that the positively charged C-terminal tail of CRT3 is crucial for its ''bri1–9-retainer'' function. Our study revealed not only a functional role for a plant-specific CRT, but also functional diversity among the 3 Arabidopsis CRT paralogues.

BRI1 | calnexin | ER chaperone | ER quality control | UGGT

Calreticulin (CRT) is a highly conserved Ca^{2+}-binding protein in eukaryotes that consists of 3 distinct domains: a globular N-domain, a proline-rich middle (P) domain, and a highly acidic C-terminal domain with a (K/H)DEL endoplasmic reticulum (ER) retrieval signal (1). Mammalian CRT has been implicated in more than 40 cellular processes in different subcellular compartments, including Ca^{2+} homeostasis and protein folding in the ER (1). CRT and its membrane-bound homologue calnexin (CNX) also contain a unique lectin site in their globular domains that specifically binds a mono-glucosylated glycan on newly synthesized glycoproteins, thus establishing the so-called CRT/CNX cycle. This system also includes glucosidase II and UDP-glucose:glycoprotein glucosyltransferase (UGGT) that catalyze removal and addition of the terminal glucose residue of Asn-linked glycans, respectively, to facilitate folding and quality control of glycoproteins in the ER (2). Deletion of CRT in the mouse leads to embryonic lethality along with abnormal cardiac development as a result of impaired Ca^{2+} homeostasis (3, 4).

Many plant species contain 2 or more CRTs that are members of 2 distinct CRT families: CRT1/2 and CRT3, which were thought to be duplicated before the splitting of monocots and dicots (5). Despite the fact that plant CRTs were discovered 15 years ago (6), their physiological functions remain largely unknown. Experiments using heterologous tissue cultures or *CRT*-over-expression transgenic plants implicated plant CRTs in multiple physiological processes such as defense against virus (7), plasmodesmata-mediated cellular transport (8, 9), tissue regeneration (10, 11), ER Ca^{2+} buffering (12, 13), and stress tolerance (14, 15). A recent study using a T-DNA insertional mutant suggested that the Arabidopsis CRT1, which can substitute the mammalian CRT function in cell culture, plays a role in ER stress response (16).

An Arabidopsis dwarf mutant, *bri1–9*, is an excellent genetic system in which to study plant ER quality control (17). BRI1 is a leucine-rich repeat receptor-like kinase that functions as a cell surface receptor for the plant steroid hormone brassinosteroids (BRs) (18). We have recently discovered that bri1–9, which carries a S662F mutation in its ligand-binding motif, is retained in the ER by an over-vigilant ER quality control system in Arabidopsis (17). Loss-of-function mutations in the Arabidopsis *EBS1* gene, which encodes a homologue of the mammalian UGGT thought to function as a protein folding sensor (19), significantly compromise this quality control system and suppress the dwarf phenotype of *bri1–9*.

To identify additional components involved in the ER quality control of the mutated BR receptor, we studied *ebs2* (*EMS-mutagenized bri1 suppressor 2*), which also suppresses the *bri1–9* mutation in an allele-specific manner. By using the map-based cloning approach, we discovered that *EBS2* encodes the Arabidopsis *CRT3*. Our biochemical experiments showed that CRT3 interacts with bri1–9 in a mono-glucosylation-dependent manner to retain the mutated BR receptor in the ER. Loss of CRT3 function allows substantial amount of mis-folded bri1–9 to move to plasma membrane to initiate BR signaling despite the presence of 2 other CRT paralogues and their membrane-localized homologues, CNXs, which were known to interact with bri1–9 in vivo. We therefore conclude that CRT3 functions as a key retention factor to keep bri1–9 in the folding compartment.

Results

The *ebs2* Mutation Partially Suppresses the Dwarf Phenotype of *bri1–9*. The same genetic screening that led to identification of *EBS1* uncovered the second *bri1–9* suppressor, *ebs2*. Similar to *ebs1*, *ebs2* partially suppresses multiple defects of *bri1–9* phenotypes throughout its life cycle. Compared with *bri1–9*, *ebs2–1 bri1–9* has elongated petioles and expanded rosette leaves at both seedling (Fig. 1*A*) and rosette (Fig. 1*B*) stages. At maturity, *ebs2–1 bri1–9* has an intermediate height compared with *bri1–9* and WT (Fig. 1*C*). In addition, *ebs2–1* partially rescues the short hypocotyl phenotype of *bri1–9* in the dark (Fig. 1 *D* and *E*).

***ebs2* Allele-Specifically Suppresses the *bri1–9* Mutation.** To investigate the underlying mechanism by which *ebs2* suppresses the

Author contributions: H.J. and J.L. designed research; H.J., Z.H., W.S., and J.L. performed research; H.J. and J.L. analyzed data; and H.J. and J.L. wrote the paper.

The authors declare no conflict of interest.

See Commentary on page 13151.

[1]Present address: Department of Molecular and Cellular Physiology, School of Medicine, Stanford University, Stanford, CA 94305.

[2]To whom correspondence should be addressed. E-mail: jian@umich.edu.

This article contains supporting information online at www.pnas.org/cgi/content/full/0906144106/DCSupplemental.

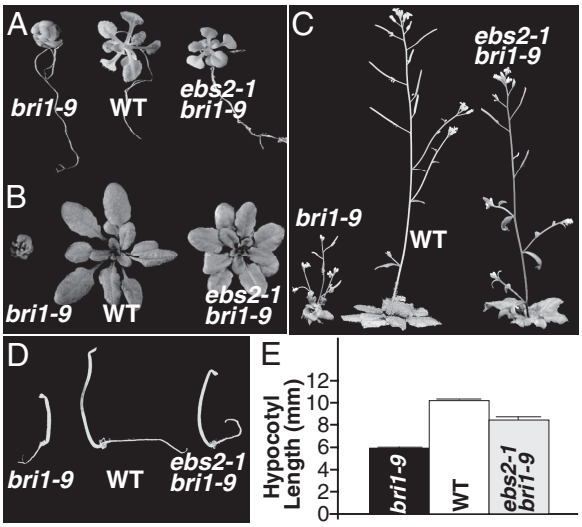

Fig. 1. The *ebs2* mutation partially suppresses the *bri1–9* mutant. Images of 7-d-old *bri1–9*, WT, and *ebs2–1 bri1–9* grown on half-strength Murashige and Skoog medium(*A*); 5-week-old soil-grown plants of *bri1–9*, WT, and *ebs2–1 bri1–9* (*B*); 7-week-old mature plants of *bri1–9*, WT, and *ebs2–1 bri1–9* grown in soil (*C*); and 4-d-old dark-grown seedlings of *bri1–9*, WT, and *ebs2–1 bri1–9* (*D*). (*E*) Average hypocotyl length of 4-d-old etiolated seedlings of *bri1–9*, WT, and *ebs2–1 bri1–9*. Each bar represents the average of more than 40 seedlings of duplicated experiments. Error bar denotes SE.

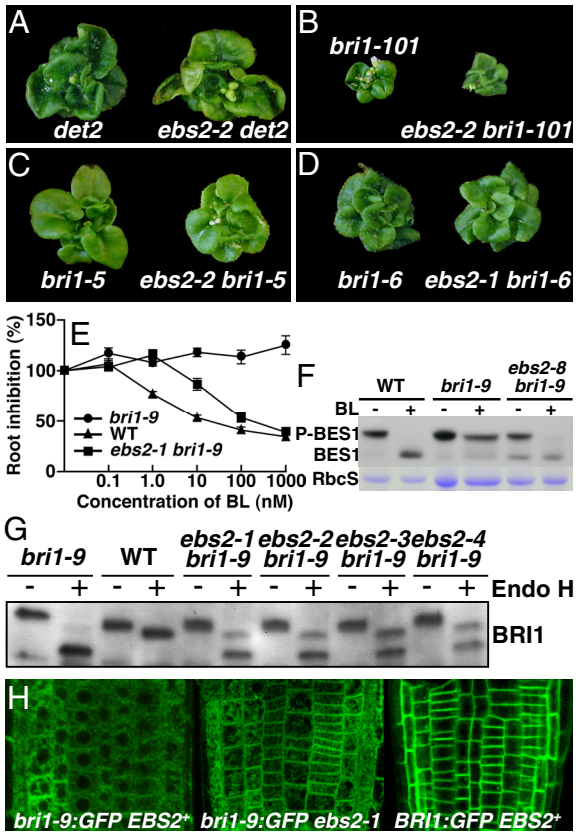

Fig. 2. EBS2 functions in quality control of bri1–9. Images of 6-week-old soil-grown *det2* and *ebs2–2 det2* mutants (*A*); 4-week-old soil-grown plants of *bri1–101* and *ebs2–2 bri1–101* (*B*); 5-week-old soil-grown *bri1–5* and *ebs2–2 bri1–5* mutants (*C*); and 5-week-old soil grown *bri1–6* and *ebs2–1 bri1–6* mutants (*D*). (*E*) Quantitative analysis of BR sensitivity. Root lengths of 7-d-old seedlings grown on BL-containing medium were measured and presented as the relative value of the average root length of BL-treated seedlings to that of mock-treated seedlings of the same genotype. Each data point represents the average of approximately 30 seedlings of duplicated experiments. Error bar denotes SE. (*F*) BR treatment leads to BES1 dephosphorylation: 2-week-old seedlings were treated with 1 μM BL for 1 h. Total proteins were extracted in 2$\times$ SDS buffer, separated by 10% SDS/PAGE, and analyzed by immunoblotting using anti-BES1 antibody (24). Coomassie blue staining of RbcS served as a loading control. (*G*) Endo H sensitivity of BRI1 and bri1–9. Equal amounts of proteins of 4-week-old leaves from different samples were treated with 1 μL of Endo Hf for 1 h at 37°, followed by Western blot analysis with anti-BRI1 antibody. (*H*) Confocal examination of subcellular localization of bri1–9:GFP and BRI1:GFP in root tips of 6-d-old light-grown seedlings.

bri1–9 phenotype, we studied the genetic interaction between *ebs2* and a BR-deficient mutant *det2* (20). As shown in Fig. 2*A*, *ebs2–2 det2* is morphologically similar to *det2*, suggesting that *ebs2* does not lead to constitutive activation of BR signaling. We also crossed *ebs2* with 3 *bri1* mutants: *bri1–101*, *bri1–5*, and *bri1–6*. The *bri1–101* contains a missense mutation in the kinase domain of BRI1 whereas *bri1–5* and *bri1–6* mutants contain mutations in their extracellular domain (21). It should be noted that bri1–5 is also retained in the ER by at least 3 retention mechanisms (22). As shown in Fig. 2 *B-D*, none of these *bri1* mutations was suppressed by *ebs2*, indicating that *ebs2* is an allele-specific suppressor of the *bri1–9* mutation. We suspected that *ebs2* might directly act on bri1–9 to restore its BR receptor function. Indeed, a BR-induced root inhibition (23) and BES1-dephosphorylation assays revealed that *ebs2* partially restores BR sensitivity to *bri1–9*. As shown in Fig. 2*E*, treatment of *bri1–9* with increasing concentrations of brassinolide (BL), the most active BR, had little effect on root growth, whereas similar treatments clearly inhibited root growth of *ebs2–1 bri1–9* and WT. Fig. 2*F* revealed that 1 h BL treatment resulted in complete and near-complete dephosphorylation of BES1, a robust biochemical marker for BR signaling (24), in WT and *ebs2–8 bri1–9*, respectively, whereas significant amounts of phosphorylated BES1 were still present in *bri1–9*.

***ebs2* Mutations Compromise the ER Retention of bri1–9.** These genetic and physiological behaviors of *ebs2* were strikingly similar to those of *ebs1* (17), implying that EBS2 might also be involved in the quality control of bri1–9. To directly test this possibility, we examined endoglycosidase H (Endo H) sensitivity of bri1–9 protein from *ebs2–1 bri1–9* and 3 other allelic *ebs2 bri1–9* mutants. Endo H removes high-mannose-type glycans of ER-localized glycoproteins but cannot cleave Golgi-processed glycans (25), thus providing a convenient way to examine the subcellular distribution of bri1–9. As shown in Fig. 2*G*, bri1–9 is sensitive whereas BRI1 is largely resistant to Endo H. Consistent with our hypothesis, a significant pool of Endo H-digested bri1–9 exhibits the same mobility as the Endo-H-processed BRI1 on Western blot filter, suggesting that *ebs2* mutations reduce the stringency of quality control of bri1–9. Indeed, confocal microscopy analysis of bri1–9:GFP revealed the presence of bri1–9:GFP at the cell surface in the *ebs2–1* mutant (Fig. 2*H*). We thus concluded that EBS2 plays a key role in retaining bri1–9 in the ER.

***EBS2* Encodes Arabidopsis CRT3.** To understand the biochemical role of EBS2 in ER retention of bri1–9, we cloned the *EBS2* gene by chromosomal walking. PCR-based genetic mapping delimited the *EBS2* locus to a 150-kb region on the top of chromosome I (Fig. 3*A*). This region contains 3 annotated genes encoding putative ER chaperones, including CRT3 (*At1g08450*), BiP3 (*At1g09080*), and CRT2 (*At1g09210*). Sequencing of these genes from *ebs2–1 bri1–9* identified a single-bp substitution in *At1g08450*, which changes Ala-333 to Val in CRT3 (Fig. 3 *B* and C). The identity of *At1g08450* as *EBS2* gene was confirmed by

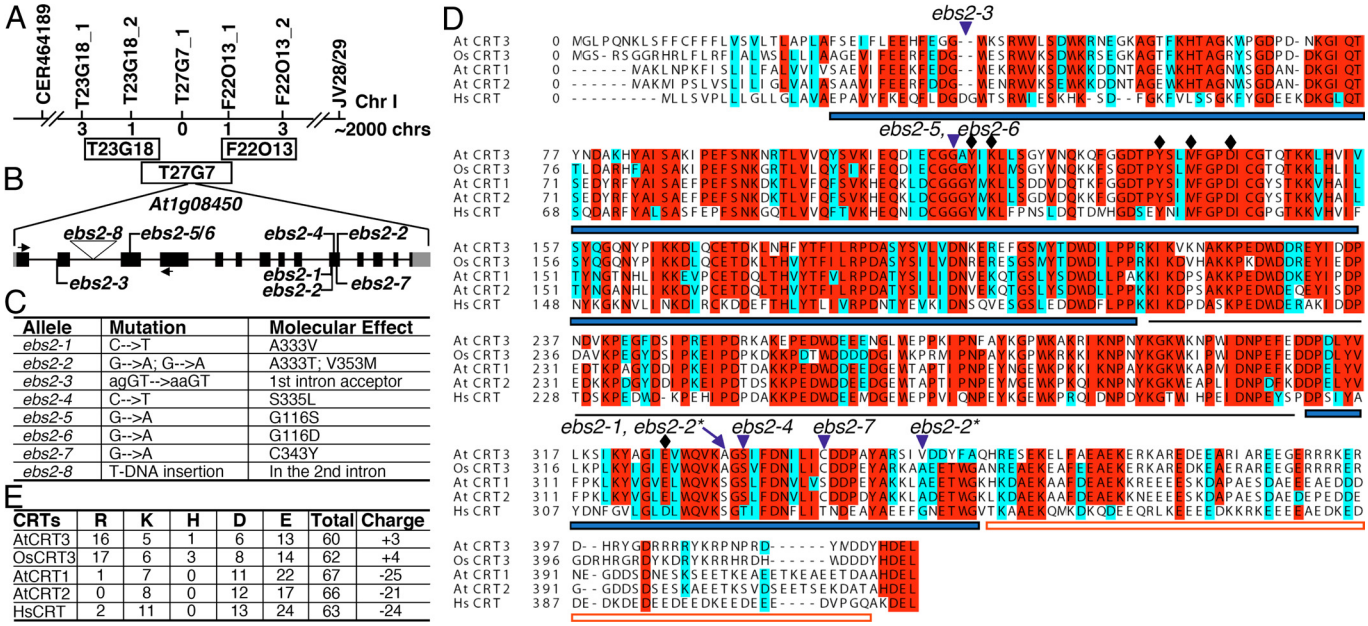

Allele	Mutation	Molecular Effect
ebs2-1	C-->T	A333V
ebs2-2	G-->A; G-->A	A333T; V353M
ebs2-3	agGT-->aaGT	1st intron acceptor
ebs2-4	C-->T	S335L
ebs2-5	G-->A	G116S
ebs2-6	G-->A	G116D
ebs2-7	G-->A	C343Y
ebs2-8	T-DNA insertion	In the 2nd intron

E

CRTs	R	K	H	D	E	Total	Charge
AtCRT3	16	5	1	6	13	60	+3
OsCRT3	17	6	3	8	14	62	+4
AtCRT1	1	7	0	11	22	67	-25
AtCRT2	0	8	0	12	17	66	-21
HsCRT	2	11	0	13	24	63	-24

Fig. 3. Molecular cloning of *EBS2*. (*A*) *EBS2* was mapped to a 150-kb genomic region between markers T23G18_2 and F22O13_1 on the top of chromosome I. The line represents genomic DNA, and markers and numbers of recombinants are shown above and below the line, respectively. (*B*) The gene structure of *EBS2*. *EBS2* contains 14 exons (black bar) and 13 introns (line). Gray boxes denote untranslated regions, lines indicate positions of *ebs2* mutations, and triangle denotes T-DNA insertion. (*C*) Nucleotide change and molecular defects of 8 *ebs2* alleles. (*D*) Alignment of CRT sequences from *Arabidopsis thaliana* (*At*), *Oryza sativa* (*Os*), and *Homo sapiens* (*Hs*). Comparison of AtCRT3 (NP_563816), OsCRT3 (BAC06263), AtCRT1 (NP_176030), AtCRT2 (NP_172392), and HsCRT (AAB51176) was performed using the ClustalW program at Network Protein Sequence analysis (http://npsa-pbil.ibcp.fr) (39). Aligned sequences were shaded using the BoxShade web server (http://bioweb.pasteur.fr). Residues identical in more than 4 sequences are shaded in red and similar ones are shaded in cyan. Each CRT contains a signal peptide, a globular domain (marked by thick blue lines), a P domain (indicated by a thin gray line), and a C-terminal domain (marked by a red open line). The positions of *ebs2* mutations are indicated by blue triangles. Stars denote 2 substitutions in *ebs2–2*, and diamonds indicate 6 residues thought to be involved in glycan binding. (*E*) Number of basic and acidic residues in C-termini [the ER retention signal (H/K)DEL was not counted] of AtCRT3, OsCRT3, AtCRT1/2, and HsCRT. The total number of amino acid residues and the net charge of these C-termini are also listed.

sequencing 6 other potential *ebs2* alleles isolated from the same genetic screen, each containing a single nucleotide change in *At1g08450* except *ebs2–2*, which carries 2 mutations, A333T and V353M (Fig. 3 *B* and *C*). In addition, a double mutant between *bri1–9* and a null T-DNA insertional mutation of *At1g08450*, named as *ebs2–8,* exhibited a suppressed-*bri1–9* phenotype that can be complemented by expression of a *CRT3* transgene containing its native promoter [supporting information (SI) Fig. S1].

CRT3 Is a Land Plant-Specific ER Lectin with a Unique Expression Pattern. The Arabidopsis contains 3 CRTs: CRT1, CRT2, and CRT3, which share similar domain organization with the rice CRT3 and the human CRT (Fig. 3*D*). Sequence comparison of the 5 CRTs revealed that, whereas they exhibit high sequence identity in the globular and P domains critical for chaperone function, the C domain of CRT3 is significantly diverged from those of CRT1 and CRT2. Unlike the C-termini of CRT1/CRT2 that are rich in acidic residues and predicted to be critical for Ca^{2+} storage (26, 27), the C-domains of 2 CRT3s are positively charged and contain short stretches of basic residues (Fig. 3 *D* and *E*). Gene co-expression analysis using ATTED-II (28) revealed that, although CRT1 and CRT2 share a similar expression profile with other ER chaperones, CRT3 is co-expressed with genes involved in plant defense and other unknown processes (Fig. S2), suggesting that the 3 Arabidopsis CRTs are involved in different physiological processes.

BLAST search and phylogenetic analysis (Fig. S3) identified CRT3s from 3 lower plant species, *Marchantia polymorpha*, *Physcomitrella patens*, and *Selaginella moellendorffii*. *Marchantia* species are members of liverworts closely related to the earliest land plants, *Physcomitrella* species are mosses thought to be the sister to all land plants except liverworts, and *Selaginella* species are considered to be the oldest living vascular plants, at approximately 420 million years old (29). Given the fact that all known CRTs from non-land-plant eukaryotes carry acidic C-termini (see http://pfam.sanger.ac.uk/family?acc=PF00262), including *Mesostigma viride* (Fig. S4), a scaly green flagellate thought to be the common ancestor of all land plants plus charophycean algae (30), our analyses suggested that the members of the CRT1/CRT2 family are more closely related to the ancestral plant CRT than the CRT3 members and that the CRT1/2-CRT3 duplication likely occurred before or during the rise of the first land plant.

CRT3 Interacts with bri1–9. The facts that mutations in CRT3 rescue the *bri1–9* phenotype and permit export of a significant amount of bri1–9 proteins out of the ER suggest that CRT3 is a major retention factor that keeps bri1–9 in the ER. However, our previous study showed that bri1–9 interacts only with CNXs but not with any of the CRTs (17) when analyzed with an anti-maize CRT antibody thought to detect all Arabidopsis CRTs and CNXs (5). We suspected that this antibody failed to detect the Arabidopsis CRT3. Indeed, Western blot analysis of T-DNA insertional mutants of 2 CNXs and 3 CRTs revealed that none of the detected CNX/CRT bands corresponds to CRT3 (Fig. S5). We therefore generated a CRT3-specific antibody (Fig. S6) to test CRT3-bri1–9 interaction with anti-GFP immunoprecipitates from transgenic plants expressing BRI1:GFP or bri1–9:GFP. As shown in Fig. 4*A*, a band corresponding to CRT3 was detected from only *bri1–9:GFP* transgenic lines, not from *BRI1:GFP* transgenic plants or WT control, indicating a CRT3-bri1–9 interaction in vivo. Such a CRT3-bri1–9 interaction likely depends on mono-glucosylation of bri1–9, as bri1–9:GFP failed to interact with CRT3 when the *bri1–9:GFP* transgene was crossed

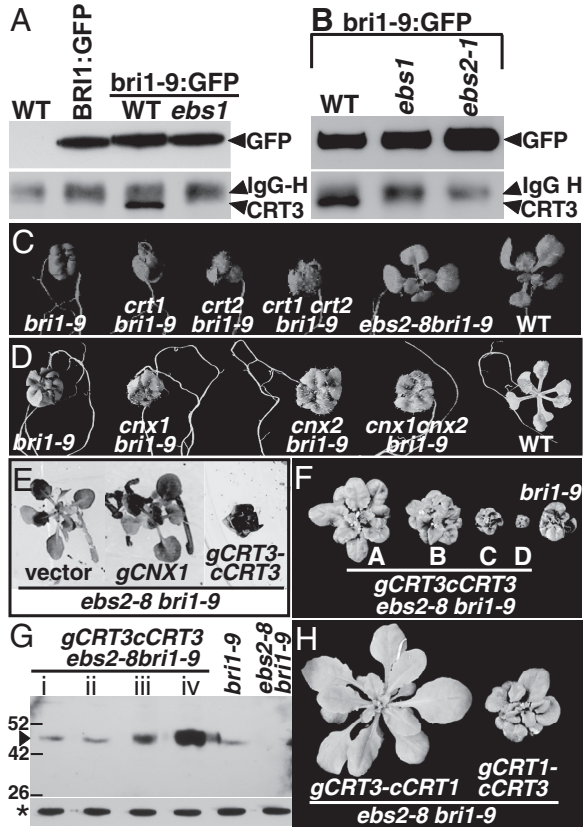

Fig. 4. CRT3 is the major lectin that retains bri1–9 in the ER. (*A*) CRT3 interacts with bri1–9 in an UGGT-dependent manner. (*B*) The CRT3-bri1–9 interaction is abolished in *ebs2–1*. For *A* and *B*, anti-GFP immunoprecipitates from 18-d-old whole seedlings of WT, or transgenic lines were separated by 10% SDS/PAGE and analyzed with anti-GFP and anti-CRT3 antibodies. IgG heavy-chain interference is indicated. (*C*) Shown here are 18-d-old seedlings of *bri1–9*, *crt1 bri1–9*, *crt2 bri1–9*, *crt1 crt2 bri1–9*, *ebs2–8 bri1–9*, and WT grown on half-strength Murashige and Skoog medium. (*D*) Shown here are 18-d-old seedlings of *bri1–9*, *cnx1 bri1–9*, *cnx2 bri1–9*, *cnx1 cnx2 bri1–9*, and WT grown on half-strength Murashige and Skoog medium. (*E*) Three-week-old transgenic *ebs2–8 bri1–9* seedlings containing *pPZP222* vector, a *gCNX1* transgene, or a *gCRT3-cCRT3* transgene. (*F*) Shown here are 6-week-old soil-grown *bri1–9* and 4 *gCRT3-cCRT3 ebs2–8 bri1–9* transgenic plants. (*G*) Analysis of CRT3 protein abundance in *gCRT3-cCRT3 ebs2–8 bri1–9* transgenic lines shown in *F*. Protein extracts of 3-week-old transgenic plants were separated by 10% SDS/PAGE and analyzed by immunoblotting with an anti-CRT3 antibody. After stripping off bound IgGs, the filter was re-probed with anti-BiP antibody. The numbers indicate molecular weight (in kDa), triangle represents CRT3, and star denotes BiP for loading control. (*H*) The C terminus is crucial for the ''retainer'' function of CRT3. Shown here are 6-week-old soil-grown transgenic *ebs2–8 bri1–9* mutants expressing the *pCRT1:gCRT1N-CRT3C* or *pCRT3:gCRT3N-CRT1C* chimeric transgene.

into *ebs1* lacking a functional UGGT that is responsible for re-glucosylating glycans on bri1–9 (17) (Fig. 4*A*).

Consistent with our finding that the suppression phenotype of *ebs2–1 bri1–9* is caused by loss of CRT3 function, the CRT3-bri1–9 interaction is abolished in bri1–9:GFP *ebs2–1* transgenic plants (Fig. 4*B*). This result suggests that Ala-333, which is changed to Val in *ebs2–1*, is important for the lectin function or proper folding of CRT3. Interestingly, the same residue is changed to Thr in *ebs2–2* that contains a second-site mutation, Val353Met. It is worth to note that most of our analyzed CRT3 sequences contain Ala at this position (Fig. S7) whereas almost all other CRTs contain a Ser residue instead (see http://pfam.sanger.ac.uk/family?acc=PF00262).

CRT3 Is the Major Lectin That Retains bri1–9 in the ER. Our discovery that CRT3 interacts with bri1–9 is quite surprising, as our previous study revealed no interaction between bri1–9 and 2 other CRTs (17) that share a highly similar globular domain involved in mono-glucosylated glycan binding (Fig. 3*D*). To eliminate the possibility that the lack of CRT1/CRT2-bri1–9 interaction might be caused by our assay condition, we crossed T-DNA insertional mutations of *crt1* and *crt2* into *bri1–9*. As shown in Fig. 4*C*, neither single nor double mutations of *crt1* and *crt2* suppresses the *bri1–9* phenotype, indicating that CRT1 and CRT2 play no role in retaining bri1–9.

Our finding that lack of CRT3 alone is sufficient to suppress the *bri1–9* phenotype to a similar extent as loss-of-function UGGT mutations is also quite puzzling. We have previously detected a strong interaction between bri1–9 and CNXs, which largely depends on mono-glucosylation of bri1–9 by UGGT (17). To test if observed CNX/bri1–9 interaction plays a role in retaining bri1–9 in the ER, we generated double and triple mutants of *bri1–9* with T-DNA insertional mutations of 2 CNXs (22). As shown in Fig. 4*D*, neither single nor double mutations of the 2 CNXs suppressed the *bri1–9* mutant. Consistent with this result, over-expression of *CNX1* by its native promoter had little effect on *bri1–9* (Fig. 4*E*). By contrast, over-expression of a CRT3 transgene with its native promoter not only rescued the T-DNA insertional mutation of CRT3 in *ebs2–8 bri1–9* but also resulted in a stronger dwarf phenotype when the CRT3 abundance was very high (Fig. 4 *F* and *G*). Taken together, our data revealed that, among the 5 CRT/CNX-type ER lectins, CRT3 plays a key role in retaining bri1–9 in the ER.

The C-Terminal Tail of CRT3 Is Critical for Its ''bri1–9 Retainer'' Function. Based on our observation that CRT3, but not CRT1/CRT2, retains bri1–9 in the ER, we suspected that the CRT3-C terminus might be important for the bri1–9 retainer function. To directly test this hypothesis, we swapped the C-termini of CRT1 and CRT3 and generated 2 chimeric transgenic constructs, *pCRT1:CRT1N-CRT3C* and *pCRT3:CRT3N-CRT1C*, driven by the native promoters of *CRT1* and *CRT3*, respectively. As shown in Fig. 4*H*, when transformed into *ebs2–8 bri1–9*, only CRT1N-CRT3C but not CRT3N-CRT1C was able to rescue the *ebs2–8* mutation. This result indicates that, although the globular and P domains of CRT1 and CRT3 are interchangeable, the CRT3 C terminus is crucial for retaining bri1–9 in the ER.

Discussion

In this study we demonstrated that the Arabidopsis CRT3, the founding member of the plant-specific CRT family, functions as a key retention factor in keeping a defective BR receptor in the ER. Results from our previous and current studies have shown that bri1–9 interacts with CNXs and CRT3 in a mono-glucosylation-dependent manner (17), yet loss-of-function mutations in CRT3 alone are sufficient to compromise the quality control of a defective BR receptor. A simple explanation for our finding is that CRT3 and CNX both retain bri1–9 in the ER, but CRT3 plays a dominant role. However, over-expression of *CNX1* failed to suppress the T-DNA insertional mutation of CRT3 in the *ebs2–8 bri1–9* mutant. We thus hypothesize that CNXs and CRT3 are involved in different cellular processes, with the 2 CNXs functioning as molecular chaperones in facilitating bri1–9 folding while CRT3 serves as an obligate retention factor to keep the mis-folded bri1–9 in the ER; and that the retainer function of CRT3 can not be accomplished by the 2 bri1–9-interacting CNXs. A similar case was reported for the folding of influenza virus hemagglutinin in mammalian cells that employ CNX for folding but use CRT for retention (31). The exact functional consequence of CNXs-bri1–9 interaction needs further investigation, and a quadruple mutant of *bri1–9 crt3 cnx1 cnx2* might be useful for such an investigation.

The most surprising discovery of our study is the functional diversification of the 3 CRT paralogues in Arabidopsis. Despite sharing a highly similar lectin-binding domain with CRT3,

neither CRT1 nor CRT2 interacts with bri1–9 in our co-immunoprecipitation assay. One possible explanation is that CRT1 and CRT2 have different client preference than CRT3. Previous studies on mammalian CRT/CNX seem to support this explanation. It is well known that mammalian CRT and CNX share the same binding specificity toward mono-glucosylated glycan in vitro but have overlapping yet distinct client proteins in vivo (32). Such client specificity is thought to be caused largely by different sub-organelle localizations of the 2 ER lectins, with CNX sitting on the ER membrane and CRT being an ER luminal protein. It was shown that ER membrane-localized CRT exhibits a similar client preference as CNX, whereas a luminal CNX shares a similar pool of client substrates with CRT (33, 34). The positively charged C-terminal tail of CRT3 might be important for a unique sub-organelle localization pattern for CRT3 to facilitate CRT-bri1–9 interaction. Consistent with this hypothesis, a CRT1-CRT3 chimeric lectin is able to complement the *ebs2–8* mutation. It is also possible that plants have evolved different CRT isoforms to participate in distinct cellular processes while the animal CRT had successfully evolved into a truly multifunctional protein. Members of the CRT1/2 family might be important for ER Ca^{2+} homeostasis as a result of their acidic C-terminal tails containing low-affinity/high-capacity Ca^{2+}-binding sites whereas CRT3 is mainly responsible for retaining mis-folded glycoproteins in the folding compartment, especially when plants are under various stress conditions in a terrestrial habitat. Consistent with this hypothesis, plant CRTs were known to affect ER Ca^{2+} levels both in vitro and in vivo and that the Arabidopsis CRT1 was recently shown to rescue Ca^{2+} deficiency of the mouse CRT-depleted embryonic fibroblasts (16). In addition, gene co-expression analysis revealed that, whereas CRT1/2 are co-expressed with many other ER chaperones, CRT3 is clustered with genes involved in stress resistance (Fig. S2). Further investigation using T-DNA insertional mutants of these ER-localized lectins could lead to a better understanding of physiological functions of plant CRT paralogues.

Materials and Methods

Plant Materials and Growth Conditions. *Arabidopsis* ecotype Columbia-0 (Col-0) is the parental line for mutants and transgenic plants with the following exceptions: *bri1–9* [Wassilewskija (Ws-2)] used for cloning *EBS2* and *bri1–5* (Ws-2) and *bri1–6* (Enkheim) used for genetic analysis. The T-DNA insertional mutants of *CRT3* (SALK_051336), *CNX1* (SALK_083600), *CNX2* (SALK_044381), *CRT1* (SALK_142821), and *CRT2* (SALK_062083) were obtained from the Arabidopsis Biological Resource Center at Ohio State University. Methods for seed sterilization and conditions for plant growth were described previously (35).

Plasmid Construction and Generation of Transgenic Plants. Transgenic plants expressing BRI1:GFP and bri1–9:GFP were previously described (17). The *CNX1* gene was amplified from genomic DNA of WT plants and cloned into *pPZP222* (36) to generate *pPZP222-gCNX1*. A 3.5-kb genomic fragment containing a 900-bp native promoter and a 400-bp cDNA fragment of *CRT3* were cloned into a modified *pPZP222-E9* vector that carries a terminator sequence of the pea *RbcS E9* gene to create *pPZP222-pCRT3::gCRT3-cCRT3* plasmid. PCR amplified genomic fragments of *CRT3* and *CRT1* carrying their promoter sequence were fused with cDNA fragments of CRT1 and CRT3 encoding their C-termini, respectively (see Table S1 for primer sequences), into *pZPZ222-E9* to generate *pPZP222-pCRT3::gCRT3-cCRT1* and *pPZP222-pCRT1::gCRT1-cCRT3* plasmids. These plasmids were then transformed into *ebs2–8 bri1–9* by *Agrobacterium* species-mediated vacuum infiltration (37).

Map-Based Cloning of *EBS2*. The *ebs2–1 bri1–9* was crossed with *bri1–9* (Ws-2) and the resulting F1 plants were self-fertilized. PCR-based genetic mapping with DNAs of approximately 1,000 F2 *ebs2–1 bri1–9* seedlings and molecular markers listed in Table S1 located the *EBS2* locus to a 150-kb region on the top of chromosome I. Three ORFs (*At1g08450*, *At1g09080*, and *At1g09210*) were independently amplified from *ebs2–1 bri1–9*, sequenced, and compared with the published sequences of WT Col-0. Several other *ebs* mutants similar to *ebs2–1 bri1–9* were crossed with *bri1–9* (Ws) and approximately 50 to 100 F2 *ebs2 bri1–9*-like seedlings for each cross were used to estimate the position of each *EBS* locus. Genomic DNAs of *ebs* mutants with their *EBS* loci mapped near *EBS2* were used to amplify *At1g08450* and the resulting PCR fragments were sequenced to determine if they carry single-nucleotide change in *EBS2*.

Endo H Treatment. Leaves from 4-week-old plants were homogenized in ''Tris, NaCl, EDTA and Triton X (TSEX) buffer'' (50 mM Tris pH 8.0, 100 mM NaCl, 5 mM EDTA, 0.2% Triton X-100, 10% glycerol, and protease inhibitors). After centrifugation, the protein extracts were denatured at 95 °C for 10 min in 1× denaturing buffer, and incubated with or without 1,000 U of Endo Hf (New England Biolabs) in the G5 buffer for 1 h at 37 °C. The treated proteins were separated by 7% SDS/PAGE and analyzed by Western blotting with anti-BRI1 serum.

Anti-CRT3 Antibody Generation. A 123-bp cDNA fragment encoding the C-terminal 41 aa of Arabidopsis CRT3 (AtCRT3) was inserted into pGEX-KG (38). The plasmid was expressed in Rosetta cells (Novagen) and the GST-CRT3C41 fusion protein was purified using glutathione Sepharose 4B-based affinity chromatography (Amersham Biosciences). The eluent was separated by SDS/PAGE and the GST-CRT3C41 band was excised and sent to Pacific Immunology for antiserum production. The anti-CRT3 specific antibody was purified using proteins bound to nitrocellulose filters modified from the procedure of Chin-Sang (http://130.15.90.245/antibody_purification.htm).

Co-Immunoprecipitation and Western Blot Analysis. A total of 0.2 g of 3-week-old seedlings were ground in liquid N_2 and extracted with the TSEX buffer. The entire procedure was conducted at 4 °C. After centrifugation at 5,000 × *g* for 10 min, the supernatant was incubated with anti-GFP antibody (TP401; Torrey Pines Biolabs) for 1 h and precipitated with protein A agarose beads (Invitrogen) for 1 h. The immunoprecipitates were washed 3 times with the TSEX buffer, separated by 7.5% SDS/PAGE, and analyzed by Western blotting using anti-GFP (MMS-118P; Covance), anti-maize CRT, or anti-CRT3 antibody. For the latter 2 antibodies, the HRP-conjugated anti-rabbit IgG light-chain antibody (Jackson Immunology) was used as the secondary antibody to avoid interference from IgG heavy chain. For other Western blot experiments, total proteins of 3-week-old seedlings were extracted with 2× SDS buffer, separated by 10% SDS/PAGE, and analyzed with anti-BES1 (24), anti-CRT3, or anti-BiP (SPA-818; Stressgen) antibody.

Bioinformatics and Phylogeny Analysis. A total of 38 unique protein sequences were aligned using a ClustalW program on the Network Protein Sequence analysis Web site (http://npsa-pbil.ibcp.fr) (39). The human CRT sequence (HsCRT) was used as the out group to root the tree. The phylogeny was constructed by using the Phylogeny Inference Package tools (http://evolution.genetics.washington.edu/phylip.html). Briefly, ClustalW alignment was analyzed using PRODIST and NEIGHBOR programs. Bootstrap assessment of tree topology derived from neighbor-joining analysis was performed 100 bootstraps with the SEQBOOT program. The derived consensus tree was displayed with the TreeView program. Bootstrap values were shown at the nodes, indicating how many times the sequences to the right of the node occurred in the same group, among 100 trees.

Confocal Microscopy. The sub-cellular localization of BRI1:GFP and bri1–9:GFP was examined by imaging root tips of 6-d-old seedlings of *BRI1:GFP*, *bri1–9:GFP*, and *bri1–9:GFP ebs2–1* transgenic lines using a Zeiss LSM510 confocal microscope filtered with FITC10 set (excitation of 488 nm with emissions of 505–530 and 530–560 nm).

ACKNOWLEDGMENTS. We are grateful to the RIKEN BioResource Center for supplying a *CRT3* cDNA plasmid, the Arabidopsis Biological Resource Center at Ohio State University for supplying cDNA/genomic clones and T-DNA insertional mutants of Arabidopsis CRTs/CNXs, F. Tax for seeds of *bri1–9* (Ws-2) and *bri1–5*, J. Chory for anti-BRI1 antibody, Y. Yin for anti-BES1 antibody, and R. Boston for anti-maize CRT serum. We thank Drs. A. Chang, S. Clark, C. Duan, M. Uhler, Y. Wang, and Y.-L. Qiu, plus members of the Li lab, for helpful discussions. This work was supported by National Institutes of Health Grant GM060519 (to J.L.).

1. Michalak M, Groenendyk J, Szabo E, Gold LI, Opas M (2009) Calreticulin, a multi-process calcium-buffering chaperone of the endoplasmic reticulum. *Biochem J* 417:651–666.
2. Caramelo JJ, Parodi AJ (2008) Getting in and out from calnexin/calreticulin cycles. *J Biol Chem* 283:10221–10225.
3. Guo L, et al. (2002) Cardiac-specific expression of calcineurin reverses embryonic lethality in calreticulin-deficient mouse. *J Biol Chem* 277:50776–50779.
4. Mesaeli N, et al. (1999) Calreticulin is essential for cardiac development. *J Cell Biol* 144:857–868.

5. Persson S, et al. (2003) Phylogenetic analyses and expression studies reveal two distinct groups of calreticulin isoforms in higher plants. *Plant Physiol* 133:1385–1396.
6. Crofts AJ, Denecke J (1998) Calreticulin and calnexin in plants. *Trends Plants Sci* 3:396–399.
7. Chen MH, Tian GW, Gafni Y, Citovsky V (2005) Effects of calreticulin on viral cell-to-cell movement. *Plant Physiol* 138:1866–1876.
8. Baluska F, Samaj J, Napier R, Volkmann D (1999) Maize calreticulin localizes preferentially to plasmodesmata in root apex. *Plant J* 19:481–488.
9. Laporte C, et al. (2003) Involvement of the secretory pathway and the cytoskeleton in intracellular targeting and tubule assembly of Grapevine fanleaf virus movement protein in tobacco BY-2 cells. *Plant Cell* 15:2058–2075.
10. Jin ZL, et al. (2005) Over-expression of Chinese cabbage calreticulin 1, BrCRT1, enhances shoot and root regeneration, but retards plant growth in transgenic tobacco. *Transgenic Res* 14:619–626.
11. Li Z, Komatsu S (2000) Molecular cloning and characterization of calreticulin, a calcium-binding protein involved in the regeneration of rice cultured suspension cells. *Eur J Biochem* 267:737–745.
12. Persson S, et al. (2001) The Ca(2+) status of the endoplasmic reticulum is altered by induction of calreticulin expression in transgenic plants. *Plant Physiol* 126:1092–1104.
13. Wyatt SE, Tsou PL, Robertson D (2002) Expression of the high capacity calcium-binding domain of calreticulin increases bioavailable calcium stores in plants. *Transgenic Res* 11:1–10.
14. Jia XY, et al. (2008) Molecular cloning and characterization of wheat calreticulin (CRT) gene involved in drought-stressed responses. *J Exp Bot* 59:739–751.
15. Sharma A, et al. (2004) A novel interaction between calreticulin and ubiquitin-like nuclear protein in rice. *Plant Cell Physiol* 45:684–692.
16. Christensen A, et al. (2008) Functional characterization of Arabidopsis calreticulin1a: A key alleviator of endoplasmic reticulum stress. *Plant Cell Physiol* 49:912–924.
17. Jin H, Yan Z, Nam KH, Li J (2007) Allele-specific suppression of a defective brassinosteroid receptor reveals a physiological role of UGGT in ER quality control. *Mol Cell* 26:821–830.
18. Li J, Chory J (1997) A putative leucine-rich repeat receptor kinase involved in brassinosteroid signal transduction. *Cell* 90:929–938.
19. Parodi AJ (2000) Protein glucosylation and its role in protein folding. *Annu Rev Biochem* 69:69–93.
20. Li J, Nagpal P, Vitart V, McMorris TC, Chory J (1996) A role for brassinosteroids in light-dependent development of Arabidopsis. *Science* 272:398–401.
21. Vert G, Nemhauser JL, Geldner N, Hong F, Chory J (2005) Molecular mechanisms of steroid hormone signaling in plants. *Annu Rev Cell Dev Biol* 21:177–201.
22. Hong Z, Jin H, Tzfira T, Li J (2008) Multiple mechanism-mediated retention of a defective brassinosteroid receptor in the endoplasmic reticulum of Arabidopsis. *Plant Cell* 20:3418–3429.
23. Clouse SD, Langford M, McMorris TC (1996) A brassinosteroid-insensitive mutant in Arabidopsis thaliana exhibits multiple defects in growth and development. *Plant Physiol* 111:671–678.
24. Mora-Garcia S, et al. (2004) Nuclear protein phosphatases with Kelch-repeat domains modulate the response to brassinosteroids in Arabidopsis. *Genes Dev* 18:448–460.
25. Maley F, Trimble RB, Tarentino AL, Plummer TH Jr (1989) Characterization of glycoproteins and their associated oligosaccharides through the use of endoglycosidases. *Anal Biochem* 180:195–204.
26. Michalak M, Corbett EF, Mesaeli N, Nakamura K, Opas M (1999) Calreticulin: One protein, one gene, many functions. *Biochem J* 344:281–292.
27. Nakamura K, et al. (2001) Complete heart block and sudden death in mice overexpressing calreticulin. *J Clin Invest* 107:1245–1253.
28. Obayashi T, et al. (2007) ATTED-II: a database of co-expressed genes and cis elements for identifying co-regulated gene groups in Arabidopsis. *Nucleic Acids Res* 35:D863–D869.
29. Qiu YL, et al. (2006) The deepest divergences in land plants inferred from phylogenomic evidence. *Proc Natl Acad Sci USA* 103:15511–15516.
30. Becker B, Marin B (2009) Streptophyte algae and the origin of embryophytes. *Ann Bot* 103:999–1004.
31. Molinari M, et al. (2004) Contrasting functions of calreticulin and calnexin in glycoprotein folding and ER quality control. *Mol Cell* 13:125–135.
32. Williams DB (2006) Beyond lectins: the calnexin/calreticulin chaperone system of the endoplasmic reticulum. *J Cell Sci* 119:615–623.
33. Danilczyk UG, Cohen-Doyle MF, Williams DB (2000) Functional relationship between calreticulin, calnexin, and the endoplasmic reticulum luminal domain of calnexin. *J Biol Chem* 275:13089–13097.
34. Wada I (1995) Calnexin is involved in the quality-control mechanism of the ER. *Seikagaku* 67:1133–1137.
35. Li J, Nam KH, Vafeados D, Chory J (2001) BIN2, a new brassinosteroid-insensitive locus in Arabidopsis. *Plant Physiol* 127:14–22.
36. Hajdukiewicz P, Svab Z, Maliga P (1994) The small, versatile pPZP family of Agrobacterium binary vectors for plant transformation. *Plant Mol Biol* 25:989–994.
37. Bechtold N, Pelletier G (1998) In planta Agrobacterium-mediated transformation of adult Arabidopsis thaliana plants by vacuum infiltration. *Methods Mol Biol* 82:259–266.
38. Guan KL, Dixon JE (1991) Eukaryotic proteins expressed in Escherichia coli: An improved thrombin cleavage and purification procedure of fusion proteins with glutathione S-transferase. *Anal Biochem* 192:262–267.
39. Combet C, Blanchet C, Geourjon C, Deleage G (2000) NPS@: Network protein sequence analysis. *Trends Biochem Sci* 25:147–150.